KANSAS CITY NSC National Security Campus

Porous Polymeric Materials

NSC-614-5683 10/2023
Unclassified Unlimited Release

FY24 PDRD Final Report

Kansas City National Security Campus

Laura Cummings
Department 896

NSC-614-5683

Distributed October 2023

Final Report

NSC-614-5683 10/2023
Unclassified Unlimited Release

PATENT CAUTION

This report may contain patentable subject matter. The contents must not be divulged outside of the Department of Energy without the approval of the Public Affairs Officer, Honeywell Federal Manufacturing & Technologies. Approved external recipients must not divulge the information to the public.

DISCLAIMER

REPRODUCTION NOTICE

The Department of Energy’s Kansas City National Security Campus is operated and managed by Honeywell Federal Manufacturing & Technologies, LLC under contract number DE-NA0002839.

Honeywell Federal Manufacturing & Technologies
14520 Botts Road
Kansas City, Missouri 64147

Contents

Illustrations

Tables

Number *Page*

1 Abstract

Fillers and pore formers are used in many materials at Kansas City National Security Campus (KCNSC) to fine tune density and stiffness. Current off-the-shelf options such as urea and Expancel do not always provide the desired properties. This project investigated several methods for introducing porosity in rigid polymers such as epoxy and polyurethane. This work was done at partnering universities to identify a variety of methods to create porous polymeric materials. The University of Oklahoma (OU) investigated emulsion templating of epoxy, where the epoxy is mixed with a surfactant and water to form an emulsion. The emulsion is then molded and cured. During the cure process, water droplets evaporate to form porous structures. Total porosity can be tuned by changing the concentration of water added to the polymer. The University of Kansas (KU) investigated the synthesis of phenolic microballoons by spray drying, as well as methods of incorporating removable porogens into epoxy and polyurethane materials to create polymeric foams.

2 Summary

This project investigated several methods for introducing porosity in polymers. All work was done at partnering universities to identify a variety of methods to create porous polymeric materials.

The University of Oklahoma investigated an emulsion templating approach where epoxy is mixed with a surfactant and water to form an emulsion. The emulsion is then molded and cured. During the cure process, water droplets evaporate to form porous structures. Total porosity can be tuned by changing the concentration of water added to the polymer. Different epoxy formulations were investigated. It was found that the order in which Part B is added plays an important role in achieving successful emulsions. Meaningful open and closed cell porous structures were only achieved after the protocol was changed to adding Part B in the final step. Additionally, using a low-viscous resin in INF-114 yielded open cell foams as opposed to EPON 815C, which yielded closed cell foams.

The University of Kansas investigated the synthesis of phenolic microballoons by spray drying, as well as methods of incorporating removable porogens into epoxy and polyurethane materials. In a previous project, water-soluble polymers were investigated as porogens, but these materials proved difficult to fully remove, and the resulting samples experienced shrinkage. This project focused on ammonium bicarbonate (ABC), which could be removed via a bake out process. Ammonium bicarbonate was chosen for this purpose as its thermal decomposition leads to the evolution of gases such as water, carbon dioxide, and ammonia, which can leave the cured structure when it is baked to decompose the salt. The University of Kansas also investigated the synthesis of hollow phenolic microballoons by a spray drying method. This work built off a project Los Alamos National Laboratories (LANL) did with Texas Tech in the early 2000s. The spray dryer KU used had a much lower maximum temperature than the one used in the Texas Tech work. Because of this adjustment, the phenolic resin formulation and catalyst had to be made to successfully spray dry the microballoons. Using an acid catalyst and a faster curing resin, KU was able to make phenolic microballoons at the lower temperature conditions.

3 Discussion

3.1 Scope and Purpose

Additive manufacturing (AM) materials and bulk composites need tunable density and stiffness that structural porosity and existing pore formers cannot achieve, so new methods of introducing porosity into existing materials need to be developed. The objective of this activity was to develop processes for the manufacture of rigid porous polymers with different pore sizes (10-50 μm target) with very narrow size distribution for use in both AM materials and bulk composites. Materials such as epoxies or polyurethanes were investigated, with a focus on methods that require minimal post processing. Efforts looked at phenolic microballoons for AM, pore formers removable by bake out, and emulsion templating of epoxy resins.

3.2 Prior Work

This project built upon prior work completed under the Next Generation Pore Former PDRD project. The results of that project are reported in NSC-614-4854.[1]

3.3 Activity

3.3.1 Spray Drying of Hollow Phenolic Microballoons

The aim of this project was to spray dry hollow phenolic microspheres of varying shell thicknesses and tap densities. Using prior work from Texas Tech as a baseline, the first run was done using DUREZ 29353 as the resin, using the same measurements at a far lower temperature of 190 ˚C. Due to this temperature difference, along with the resin being a slower curing resin, the run was not successful. Some bench-scale experiments were done to determine curing time. Experimenting with different resins and carrier solvents led to the first successful run, which consisted of the following: DUREZ 34610 as the resin, ethanol as a carrier solvent, ABC as the blowing agent, and 3M HCl as the acid catalyst (20 wt.% of resin). After spray drying, SEM images of the obtained microspheres were taken (see Figure 1), from which a shell thickness of ~1 micron was determined. The average size from observation was 5-10 microns, with a tap density of 0.3 g/mL.

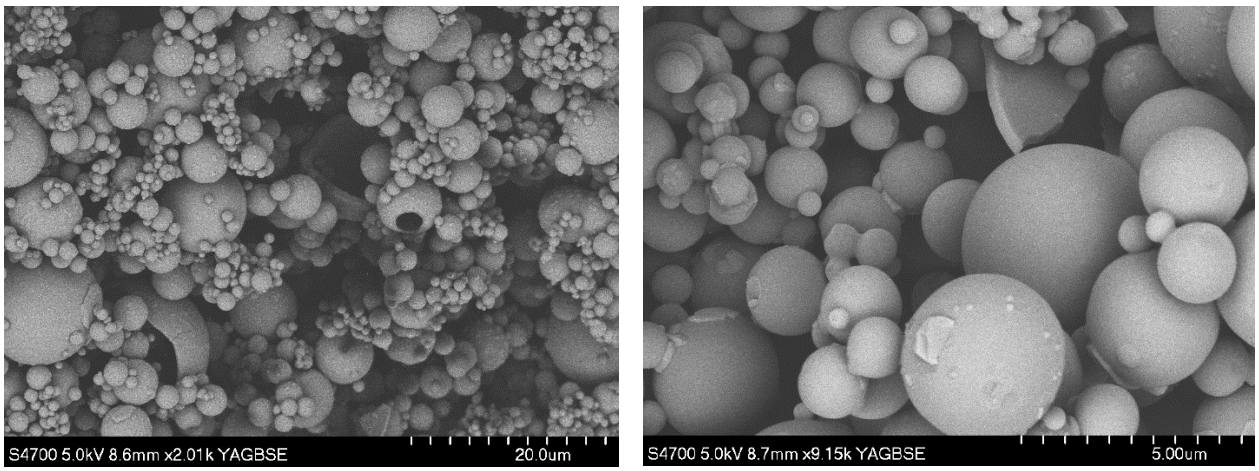

Figure 1. SEM images of spray dried phenolic microspheres

3.3.2 Ammonium Bicarbonate as Pore Former in Epoxy and Polyurethane

The focus during this fiscal year was to utilize bicarbonate salts as pore formers, specifically ABC. Ammonium bicarbonate was chosen for this purpose as its thermal decomposition leads to the evolution of gases, such as water, carbon dioxide, and ammonia, which can leave the cured structure when it is baked to decompose the salt. The reaction below shows the decomposition mentioned:

$$NH_4HCO_3 \rightarrow NH_3 + H_2O + CO_2.$$

The first incorporation of ABC was in polydimethyl siloxane (PDMS) polymers, wherein up to 80 wt.% incorporation was achieved (see Figure 2). Through mass measurements, we could determine complete loss of ABC upon baking, and the foams with higher wt.% incorporations of ABC were noticeably softer, owing to their higher porosity. SEM images revealed irregular pores left behind from removal of ABC, as seen in Figure 3.

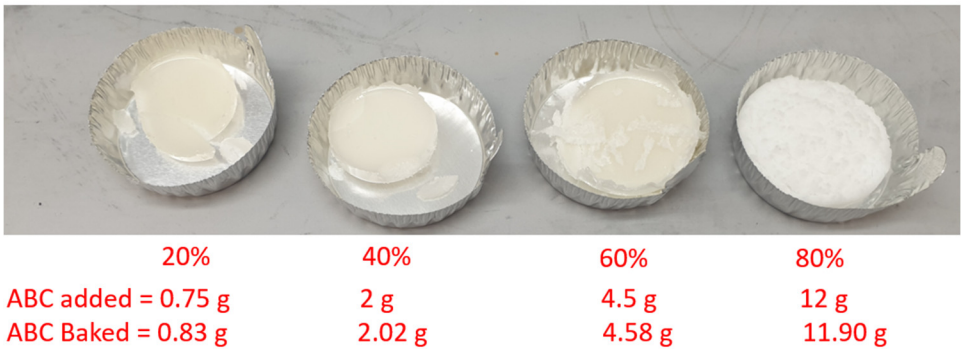

Figure 2. ABC incorporated into DMS-V51 at various loadings

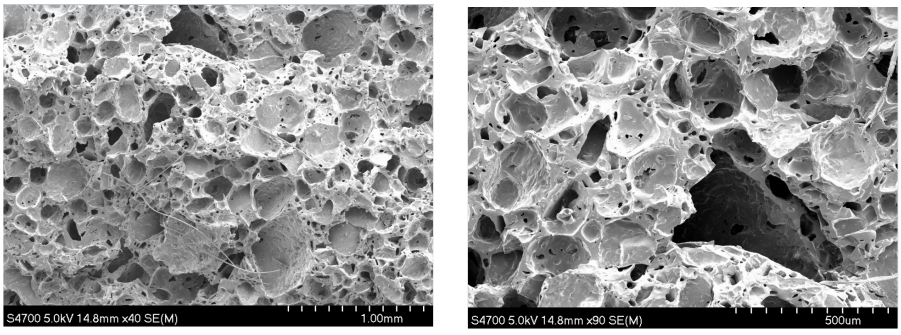

Figure 3. SEM images of DMS-V51 foam with ABC baked out

The main focus of this fiscal year was to incorporate ABC into epoxies and polyurethanes, and across the various polyurethanes and epoxies we explored, we consistently observed some degree of swelling/blowing up of the polyurethane foams. The current theory on this effect is that the free isocyanate groups within the polyurethane react with the water produced from the decomposition of ABC, leading to further formation of CO_2, which causes the swelling. This is clearly shown in the SEM images in Figure 4, wherein each image is from a different sample that used a different polyurethane as the base, yet the same effect is clearly observed in both.

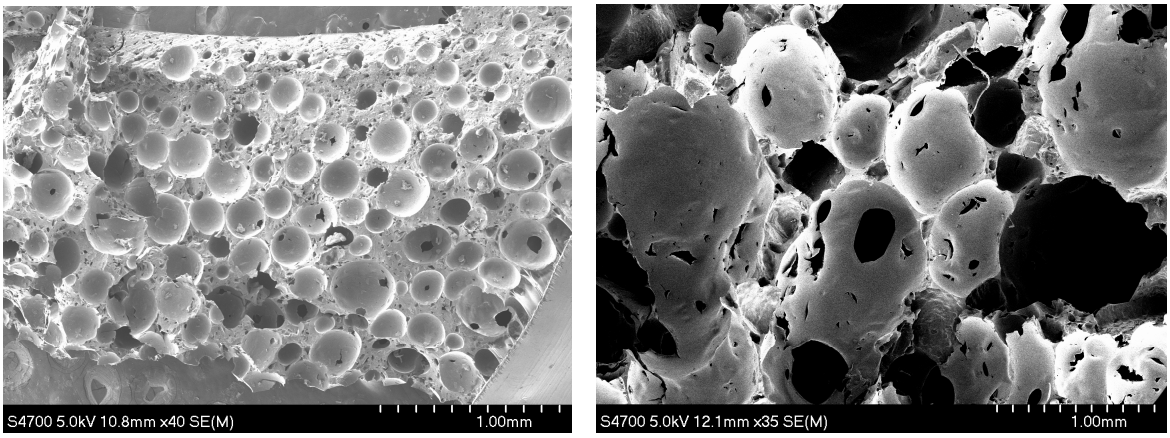

Figure 4. SEM images showing "microballoons" formed in polyurethane foams, leading to swelling

This swelling leads to the polyurethane samples being highly compressible after the ABC has been baked out, as shown in Figure 5.

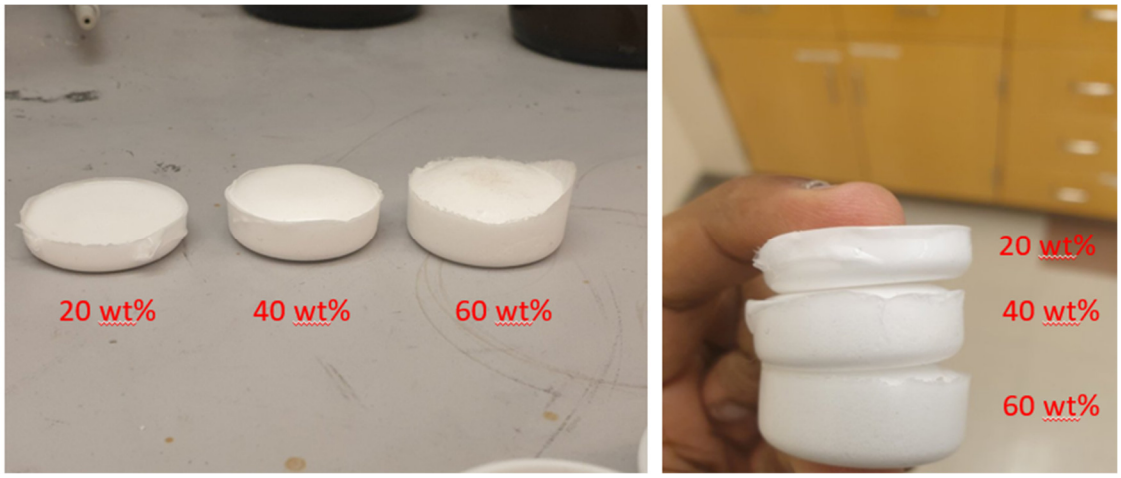

Figure 5. Polyurethane foams with different loadings of ABCG

This effect was more prominent in the ABC that was simply ground in the mortar and pestle and then incorporated (ABCG) compared to the ABC that was ground over a 45-micron sieve filter and then incorporated (ABC45S). As shown in Figure 6, high incorporations of ABC45S in polyurethanes proved to be challenging, owing to the collapse of structure post-bake.

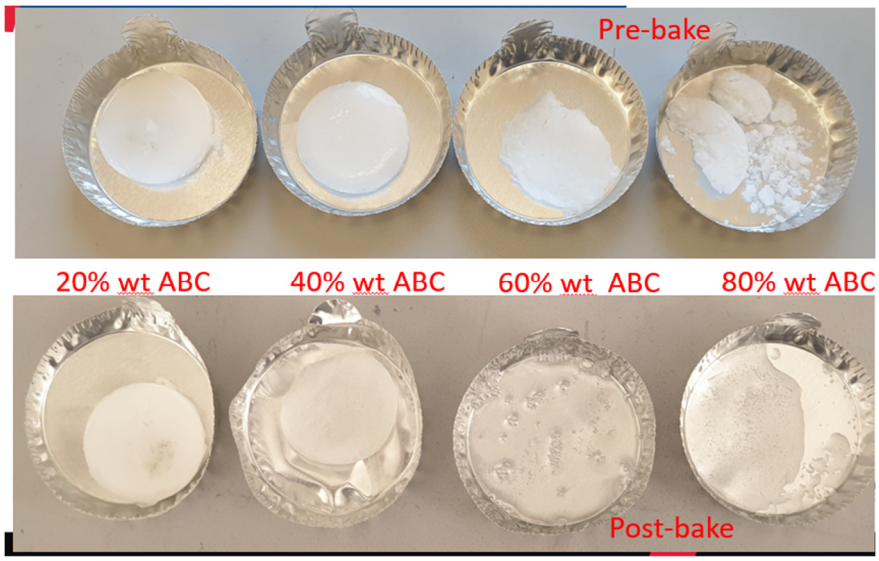

Figure 6. Polyurethane foams with different loadings of ABC45S

In contrast, the epoxy samples held well even at high loadings of ABC45S, although some shrinkage was observed at 80 wt.% (see Figure 7). The epoxy samples were more rigid and stiff in comparison to the polyurethane samples, and SEM images showed irregular voids compared to the balloon structures seen in the polyurethane samples (see Figure 8).

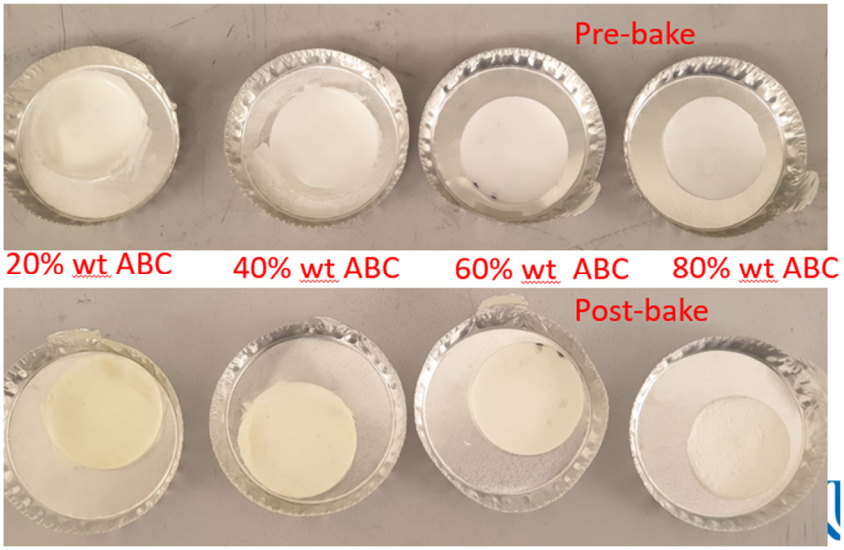

Figure 7. Epoxy foams with different loadings of ABC45S

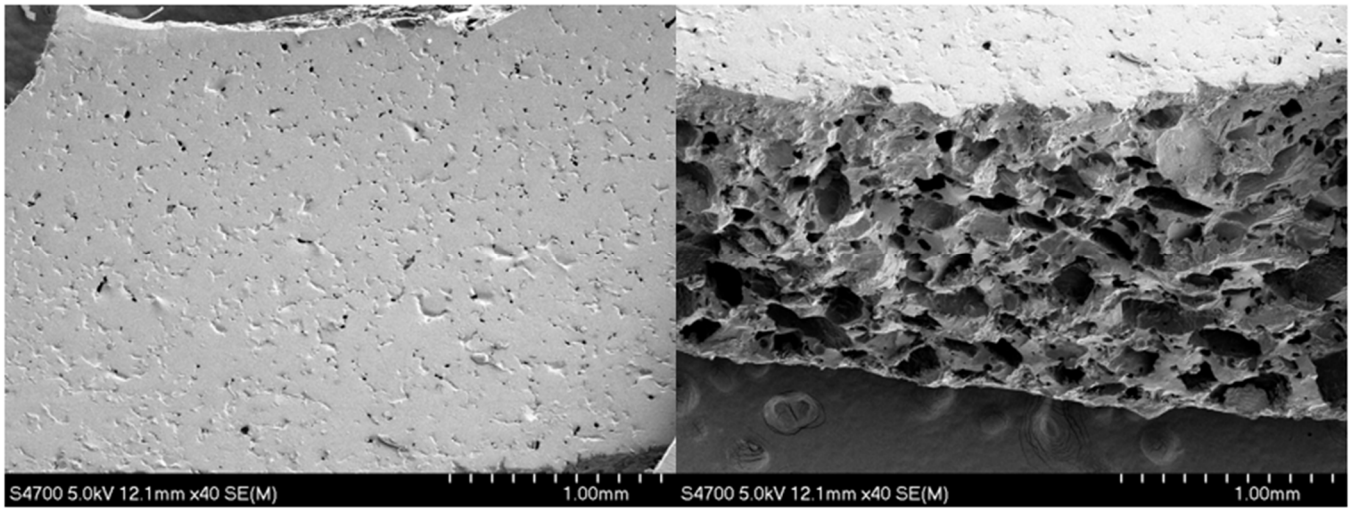

Figure 8. Epoxy foam with 50% ABCG

The swelling in polyurethane foams, while commonly observed, was not consistent in that some loadings of ABCG versus ABC45S produced different swelling effects. To learn more about this, a set of experiments was done wherein ABCG and ABC45S was incorporated into polyurethanes and epoxies at fixed loadings. Dimensions of the foams were noted pre- and post-bake to track any swelling/shrinking. These experiments were done twice to get a better understanding of trends across both polyurethane and epoxy samples.

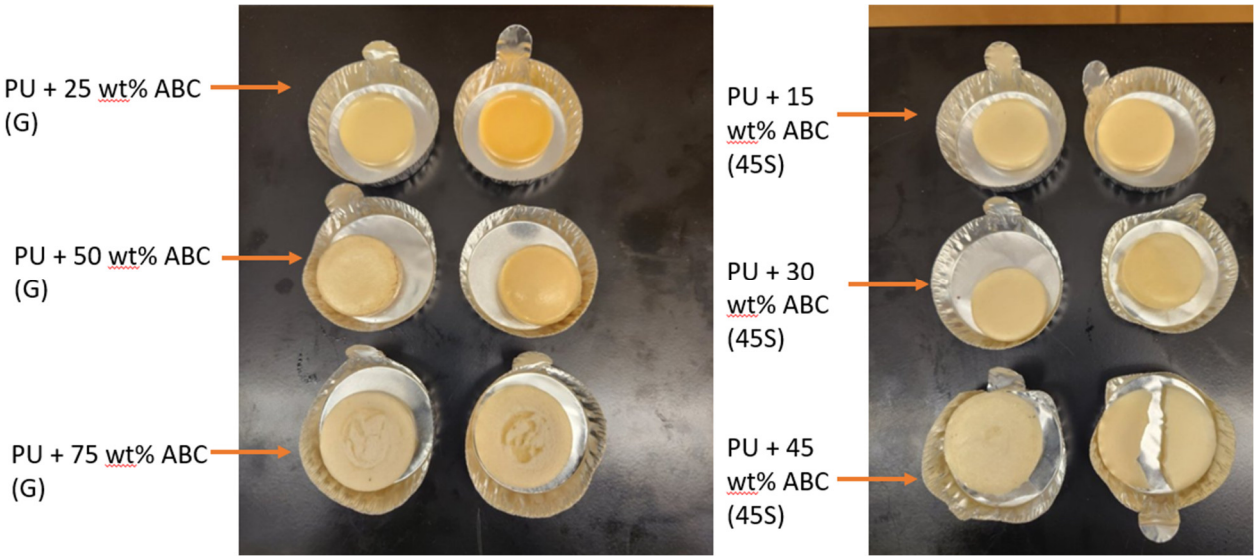

Figure 9. Polyurethane foams with different loadings of ABCG and ABC45S

The trend observed from the polyurethane samples (see Figure 9) was that for swelling, the 50 wt% ABCG showed this effect consistently and prominently (which made it the most compressible sample), while higher loadings of both ABCG and ABC45S showed shrinkage post-bake. This could be because after sieving, at the same mass loading, more volume of ABC is incorporated in ABC45S versus ABCG. Instead of causing swelling, this causes the structure to shrink due to the large void spaces left behind.

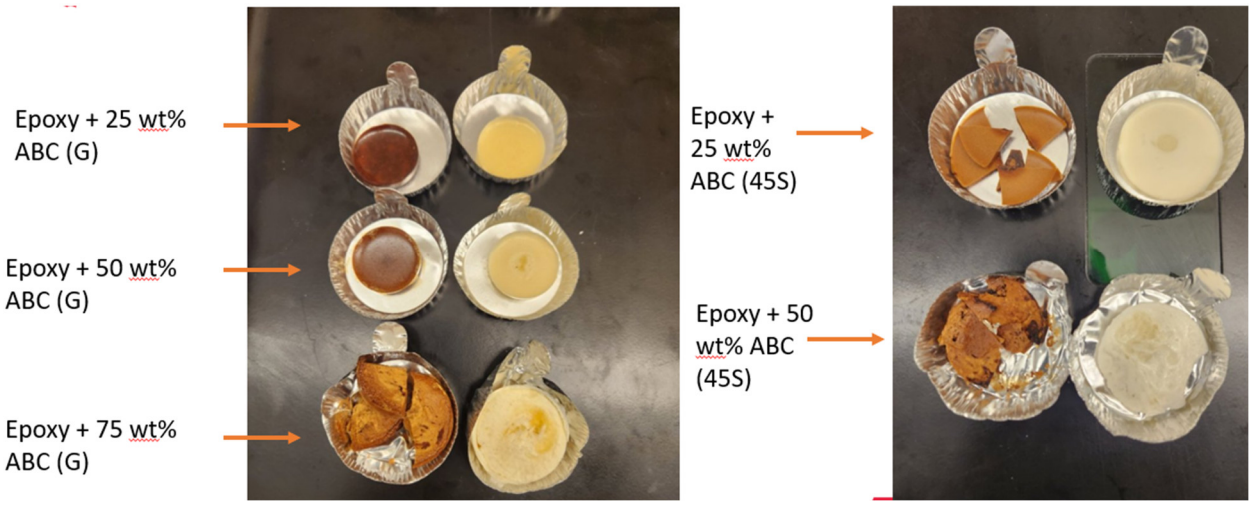

Figure 10. Epoxy foams with different loadings of ABCG and ABC45S

For the epoxy samples, there were no changes in dimensions observed pre- and post-bake, which was consistent with prior observations. The 75 wt.% ABC45S sample could not be made as there was too much ABC relative to the epoxy. The darker color of one set of samples (see Figure 10), is attributed to a longer bake time (3 days at 100 ˚C versus 1 day). The epoxy samples were also more brittle at higher loadings and did not show the same compressibility as the polyurethane samples.

Compressive modulus measurements were taken of epoxy and polyurethane samples across various loadings. The results are summarized in Table 1 and Table 2.

Table 1. Compressive modulus measurements of various epoxy samples with ABCG and ABC45S

Sample Loading	Compressive Modulus (MPa)
25 wt% ABC (G)	3.1 MPa
50 wt% ABC (G)	17.151 MPa
75 wt% ABC (G)	N/A
15 wt% ABC (45S)	17.4825 MPa
30 wt% ABC (45S)	19.178 MPa
45 wt% ABC (45S)	11.912 MPa

Table 2. Compressive modulus measurements of various polyurethane samples with ABCG and ABC45S

Sample Loading	Compressive Modulus (MPa)
25 wt% ABC (G)	0.3985 MPa
50 wt% ABC (G)	0.0885 MPa
75 wt% ABC (G)	N/A
15 wt% ABC (45S)	0.63 MPa
30 wt% ABC (45S)	0.06925 MPa

45 wt% ABC (45S)	0.0758 MPa

As illustrated by the values in Table 1 and Table 2, the polyurethane foams are 2-3 orders of magnitude softer than the corresponding epoxy foams, which is to be expected due to the isocyanate reaction with water. For the epoxy foams, the values of the ABC45S foams start out higher than those of the ABCG, even at lower loadings, which could be due to sieving introducing some level of size control. The last ABC45S sample might have a lower compressive modulus due to there being too much ABC per volume, leading to the structure not holding itself together well post-bake. For the polyurethane foams, the initial loading values start out at under 1 MPa, but from the next loading, a decrease by an order of magnitude is noted, with values being under 0.1 MPa.

3.3.3 Porous Epoxy Foams Utilizing Emulsion Templating

Emulsion templating technology is one of the most popular methods for the synthesis of porous polymers. The emulsion droplets behave as a template in this technique, and the porous polymer structure is fabricated by polymerization of the continuous phase of an emulsion, followed by the removal of the droplet phase.

In this study, we aimed to investigate the curing behavior, mechanical properties, and failure modes of EPON 815C epoxy samples, comparing results from different curing profiles and sample sizes. This was used as the building block in achieving a porous emulsion by utilizing various surfactants and colloidal silica types in stabilizing the emulsion. A comprehensive study was conducted to analyze optimizing the formulation parameters to achieve successful curing, controlled agglomeration of colloidal silica, and the development of a desired porous structure was conducted. The study also explored the impact of surfactants, water sources, and hardener variations on the curing and mechanical properties of the samples.

3.3.3.1 Materials and Fabrication

Two types of epoxy systems have been investigated for this study. The first epoxy system (EPON 815C, EPIKURE 3230, and EPIKURE 3245) was procured from Westlake. The second epoxy system (INF-114 and INF-211) was procured from Pro-Set. In that study, different surfactants were employed in stabilizing the emulsion: DOWSIL ES-5300 supplied by Honeywell and Span® 20 and Span® 80 supplied by Sigma-Aldrich. AEROSIL® 300 and R 8200, purchased from Evonik Industries, were used in conjunction with the deionized (DI) water as an internal phase and to assist in the nucleation process. In addition, TM-50 colloidal silica, supplied by Sigma-Aldrich, was employed as the internal phase. All chemicals were used as received.

Two types of samples were fabricated for characterization: solid epoxy and porous epoxy structure. For solid epoxy, epoxy and hardener were mixed manually according to the manufacturer's mixing ratio for about 3 minutes, followed by THINKY mixing on Defoamed mode for an additional 5 minutes. After mixing, the epoxy was then poured into a silicone rubber mold. A rectangular mold was used for compression samples, and a dog-bone-shaped mold was used for tension samples. The samples were placed in a vacuum chamber and degassed for 20 minutes after being poured into the silicone mold before post-curing. This was done to remove the voids induced after being poured into the silicone mold. Samples were immediately post-cured in a programmable oven at 80 °C for 2 hours, then 100 °C for 1 hour, as per the manufacturer's instruction. Schematics of the neat epoxy sample preparation procedure for both compression and tension tests are shown in Figure 11 and Figure 12.

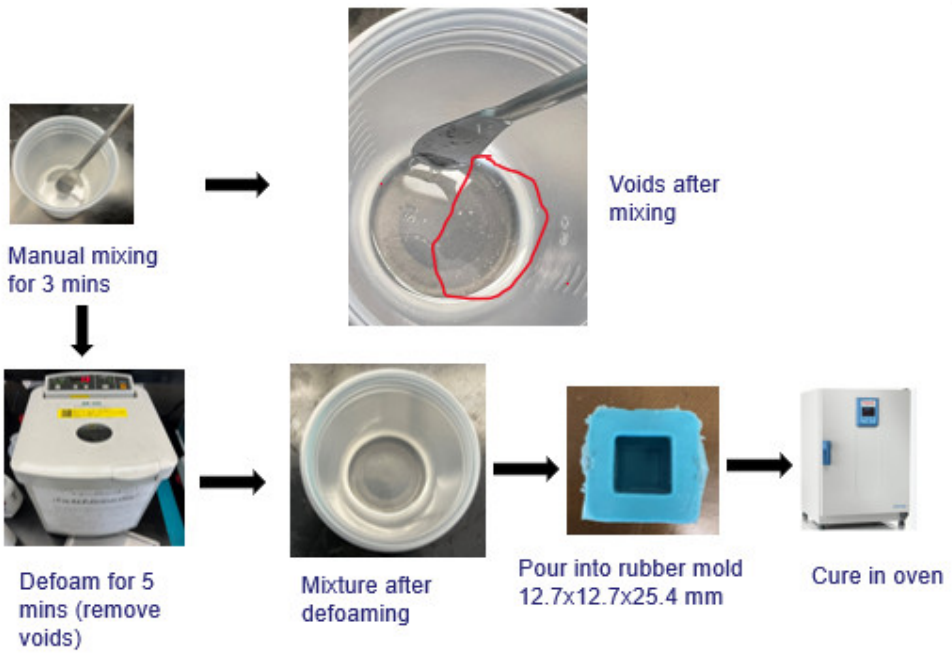

Figure 11. Neat epoxy compression sample preparation

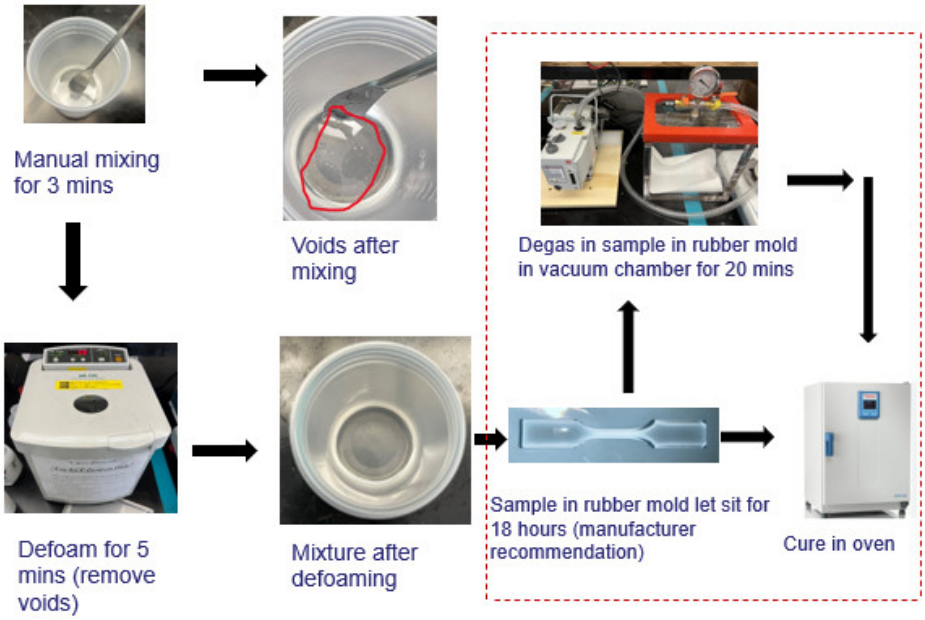

Figure 12. Neat epoxy tension sample preparation

For the porous epoxy study, emulsion templates with different formulations were investigated using two separate mixing protocols that differed in when the hardener was added (either the first step or the last step of the mixing process). Multiple analysis was conducted in this study to understand the suitable surfactant type, curing agent, amount of curing agent, resin, and internal phase content to create a stable emulsion and the porous epoxy foam with desired properties.

3.3.3.2 Characterization

Both the fracture surface and internal structure of the fabricated samples were explored by optical microscopy using a Keyence VHX-7000 ultramicroscope, which is a high magnification optical

microscope with a motorized XYZ stage, optical surface profiling, and up to 6500x magnification. For porous samples, the following equations were used to extract porosity information from some of the successfully created samples:

$$\boldsymbol{Porosity}\ (\%) = \left(\mathbf{1} - \frac{\boldsymbol{\rho_1}}{\boldsymbol{\rho_0}}\right) \times \mathbf{100} \ldots\ldots\ldots\ldots (\mathbf{1})$$

Where ρ_0 and ρ_1 are the densities of the dense polymer and porous sample, respectively.

3.3.3.3 Cure Study of Neat Epoxy

EPON 815C epoxy is a widely used material due to its mechanical properties and versatility. Understanding its curing behavior, mechanical response, and failure mechanisms is crucial for improving its application potential. This study aimed to investigate the curing behavior, mechanical properties, and failure modes of EPON 815C epoxy samples, comparing results from different curing profiles and sample sizes. The manufacturer recommended a curing profile where a programmable oven's temperature is ramped to 80 °C and held for 2 hours then ramped to 100 °C and held for 1 hour. However, a non-manufacturing profile with a lower starting temperature was investigated with the goal of future implementation for the porous epoxy foam study. Lower starting temperatures are desired to prevent the water source from the internal phase from boiling before the polymerization successfully encapsulates the water molecules. The curing profile chosen was a temperature ramp to 40 °C then held for 30 minutes, followed by a ramp to 90 °C that was held for 30 minutes.

3.3.3.4 Compression and Tensile Behavior of Neat Epoxy

According to the ASTM D695 standard, the specimen height should be twice the lateral side. As seen in Figure 13, both sets of samples failed due to global buckling, with the samples prepared using the non-manufacturer's curing cycle experiencing less failure due to buckling, as observed in its post-compressed structure. The compressive stress-strain plot for both sets of samples for the manufacturer (red) and non-manufacturer (blue) are shown in Figure 14. As shown in Figure 14, the manufacturer's curing profile showcases a higher loading capacity than the chosen non-manufacturer curing profile.

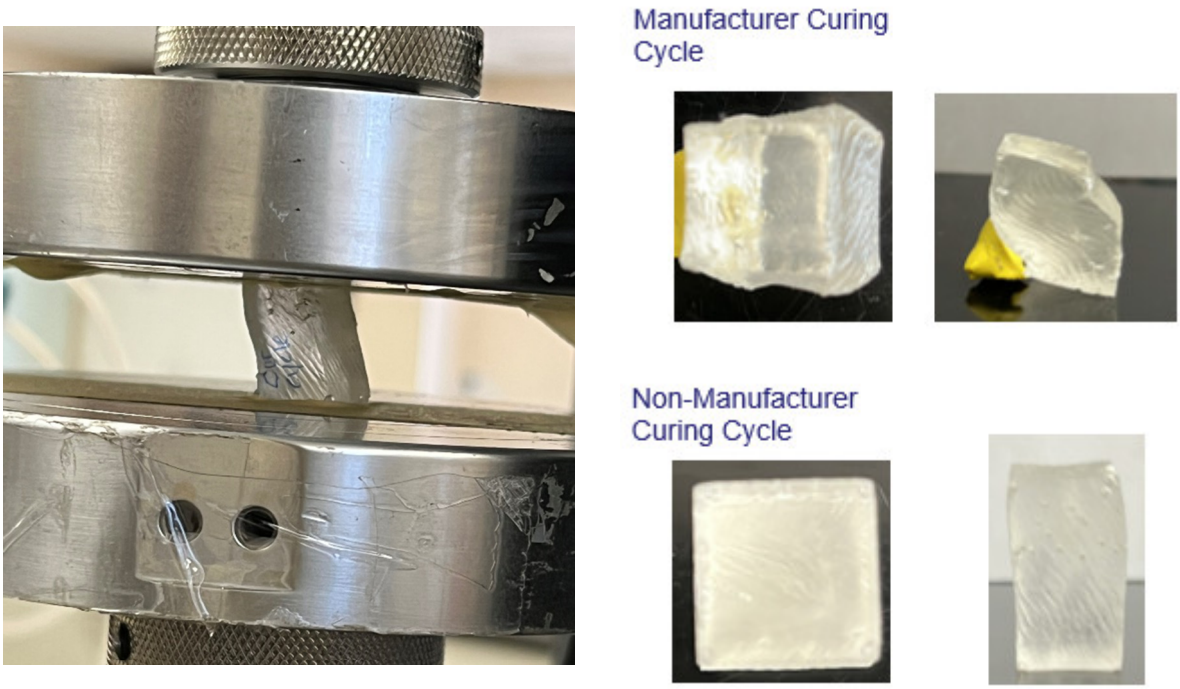

Figure 13. Compression samples during (left) and post (right) compression testing

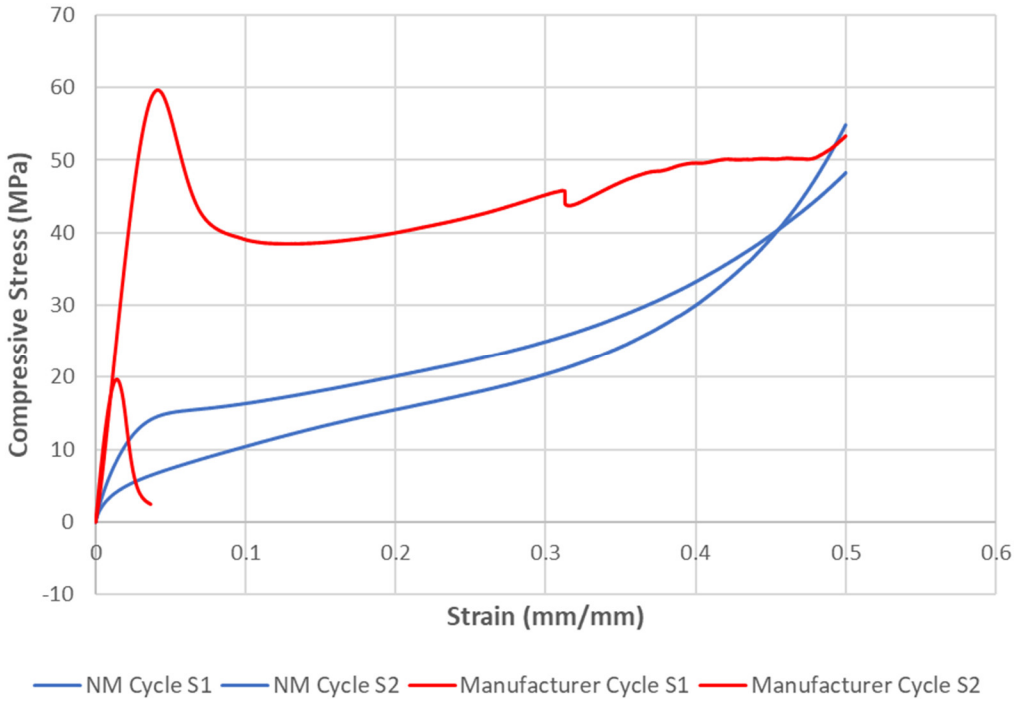

Figure 14. Compressive stress-strain plot for manufacturer and non-manufacturing curing

To solve the problem of the sample failing due to buckling, shorter samples were fabricated by cutting the original sample in half. For this purpose, new molds with a better surface finish were machined and used to create better quality silicone rubber molds that resulted in a substantial decrease in the voids on the edges of the samples and a much cleaner surface finish (see Figure 15).

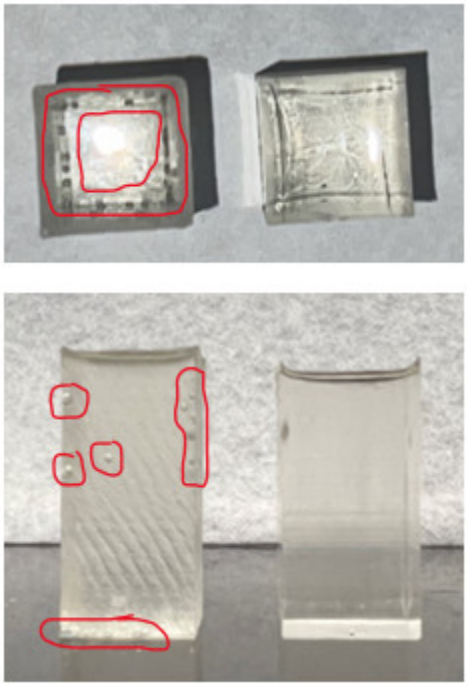

Figure 15. Compression samples were originally fabricated (left) vs. new samples made using a new mold

As shown in Figure 15, the new molds produced a much cleaner finish compared to the original fabricated samples. Once these new samples were obtained, the samples were cut into two 0.5-inch samples using a diamond cutter. As a result of the new sample length, the resulting compressed samples experienced true failure rather than failure due to buckling. The stress-strain plot for these new samples cut at a 0.5-inch mark for 8 mm deformation compression test is shown in Figure 16.

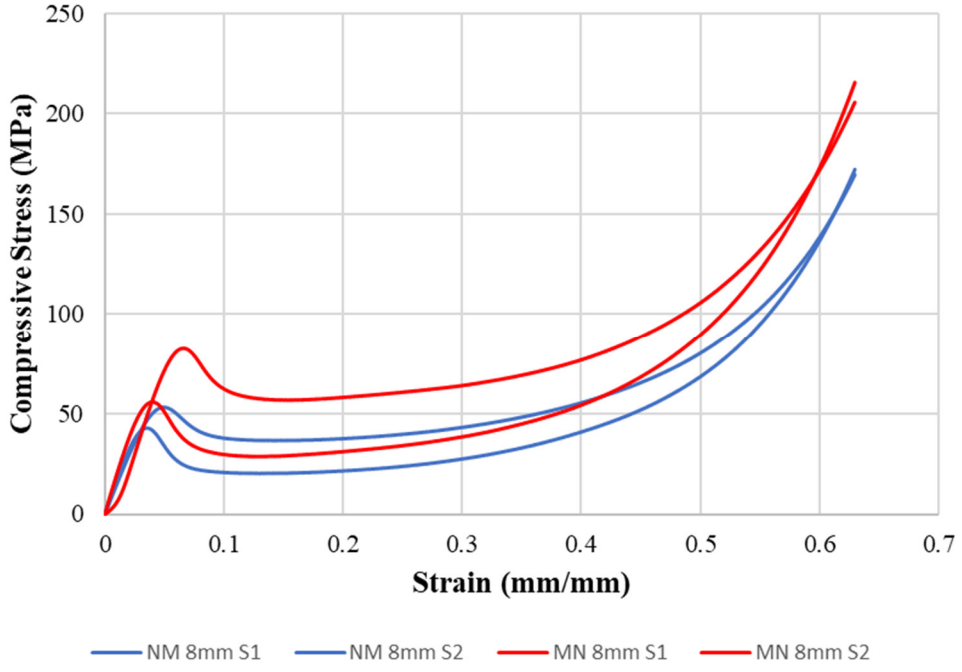

Figure 16. Compressive stress-strain plot for new samples at 8 mm deformation

The samples fabricated using the manufacturer's curing profile have consistently shown higher loading capability compared to the non-manufacturer's curing profile that was also utilized. As stated earlier, the newly cut shorter samples did not experience failure due to buckling. However, a type of crazing phenomenon was observed where microcracks appeared at high-stress concentrations (see highlighted in red in Figure 17).

Figure 17. Cut samples post compression tests and highlighted crazing

Tension tests were carried out on dog bone samples using two different strain measuring methods. The first method was the standard method using a Linear Variable Differential Transformer (LVDT) while the other method utilized the Advanced Video Extensometer (AVE). This was done to verify the modulus data with the data obtained from the material's datasheet. The tensile parameters used were a testing speed of 1 mm/min., a 5kN load cell, and specimen size with a width of 3.73 mm, thickness of 2.694 mm, and gauge length of 7.62 mm.

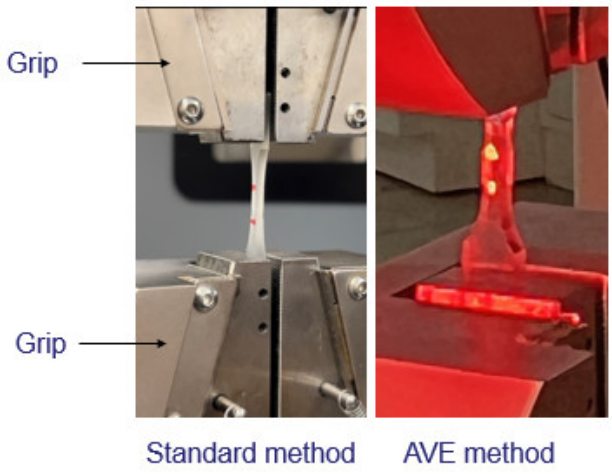

Figure 18. Standard (left) vs. AVE method (right) strain measurement methods

Figure 18 shows the different methods used for the tension tests of the samples. The tensile stress-strain plots for the tension tests are shown in Figure 19.

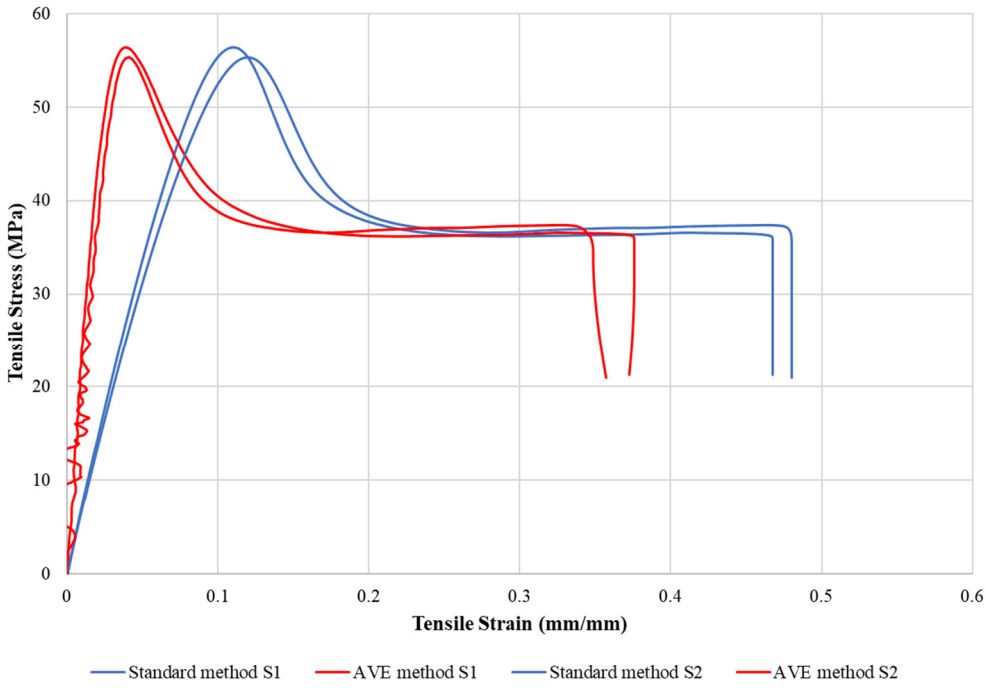

Figure 19. Tension stress-strain plot based on two different strain measurement methods

Table 3 summarizes the Young's Modulus, ultimate tensile strength (UTS), and strain at UTS data.

Table 3. Tensile modulus and UTS data

		Standard	AVE
Modulus (GPa)	S1	0.807	3.50
	S2	0.760	3.50
UTS (MPa)	S1	56.37	56.37
	S2	55.35	55.35
Strain @ UTS	S1	0.110	0.039
	S2	0.119	0.041

The tensile strength of the samples was consistent, within a reasonable margin (55–56 MPa), and greater than the reported value from the manufacturer (46–49 MPa). The modulus data using AVE yielded more accurate results compared to the manufacturer's reported value of 3.15 GPa.

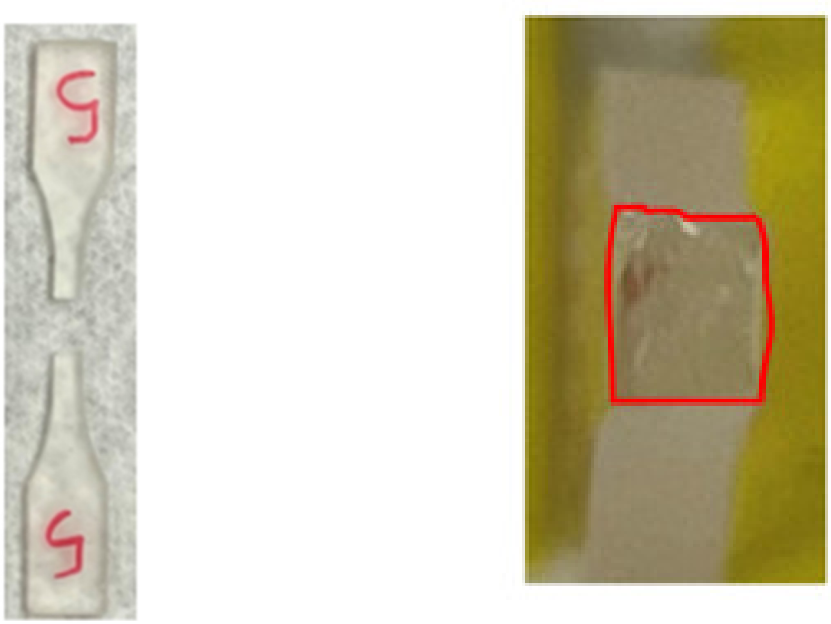

Figure 20. Tension samples post-tension tests and cross-section (right)

Figure 20 shows the dog bone sample post-tension testing. All samples failed near the gauge section. The image on the right in Figure 20 shows the cross-section of the sample showing a rougher fracture surface.

3.3.3.5 Effect of Extra Hardener

This study pursued the formulation of porous emulsions using EPON 815C epoxy. The objective was to optimize the formulation parameters to achieve successful curing, which did not occur with the initial formulation with the manufacturer's Part A:Part B weight ratio. Instead, an agglomeration of colloidal silica and no sign of the development of a desired porous structure was observed. The study also explored the impact of surfactants, water sources, and hardener variations on the curing of the samples.

Figure 21 and Figure 22 show images of the samples made according to Formulation 1, which, after adding Part A, involves adding the surfactant Span® 20 and TM-50 colloidal silica to the mixture and THINKY mixing for 5 minutes. The curing agent was then added and mixed for an additional 3 minutes.

The weight percentages of this formulation are as follows: 50% epoxy, 50% water, 5% surfactant (with total), and 100% colloidal silica (with total). The 50% water content was derived from the amount of colloidal silica utilized.

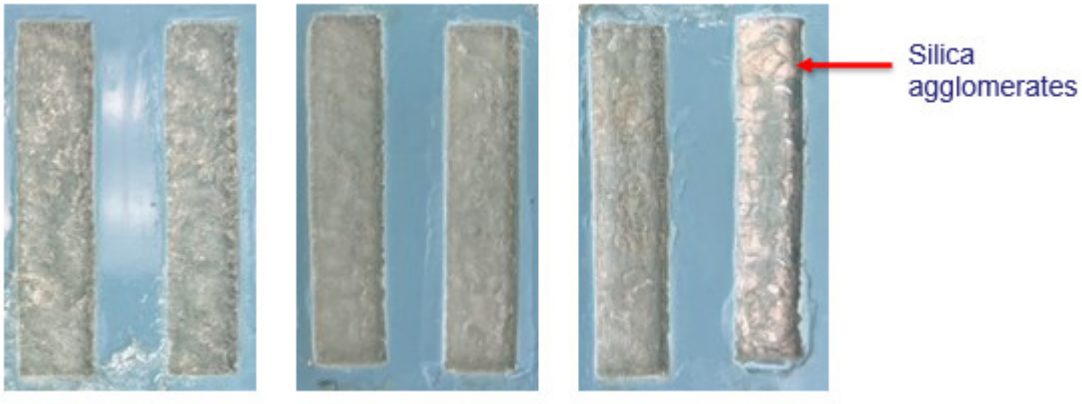

Figure 21. Formulation 1 with Span® 20 samples after oven curing with extra hardener (from left to right): 10%, 20%, and 30% extra hardener

It was observed that the samples were not cured and had a sticky texture. Water was also trapped at the bottom of the sample, and silica agglomeration was observed in samples with 30% extra hardener. Upon extending this study up to 80% extra hardener, it was found that at the 80% mark, samples completely hardened but were very brittle and crumbled easily. Samples with 80% extra hardener, although solid, do not exhibit any form of rigidity as seen with most epoxy foams. The samples with 80% extra hardener were duplicated and extended up to 100% extra hardener, which also showcased similar behavior seen with the 80% extra hardener sample. This is shown in Figure 22.

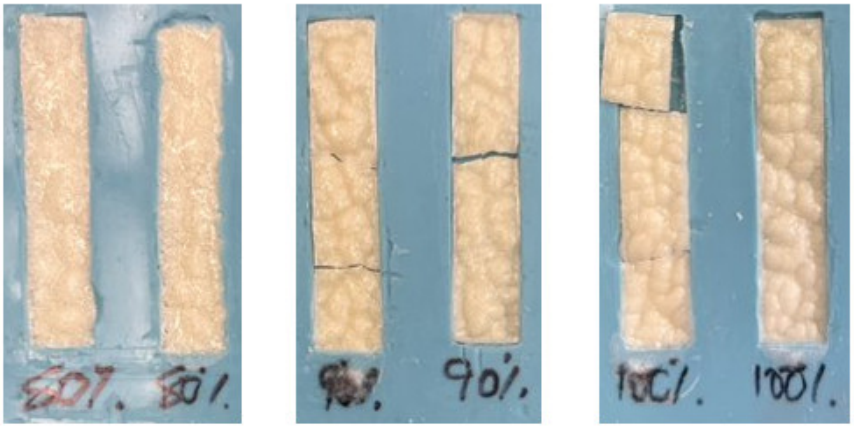

Figure 22. Formulation 1 with Span® 20 samples after oven curing with extra hardener (from left to right): 80%, 90%, and 100% extra hardener

3.3.3.6 Open Cell Foam Study

Open cell foams were observed through the fabrication process involving INF-114. This fabrication process followed Formulation 2, which, after adding INF-114 (Part A) and INF-211 (Part B), involves adding and thoroughly mixing the surfactant DOWSIL ES-5300. DI water and AEROSIL® 300 silica were then mixed separately, and small amounts (1.3–1.4 g) were added to the mixture and THINKY mixed for 25 minutes. The weight percentages of this system are consistent with Formulation 1 aside from adding

0.5% AEROSIL® 300 silica, which was used in the appropriate amount of water. The curing profile also changed as this sample was held at 82 °C for 2 hours.

This study was conducted using 10, 20, 30, 40, and 50% DI water + AEROSIL® 300 colloidal solution. The 10% sample did not exhibit any sign of porous structure. The optical images of the other resulting samples are shown in Figure 23, Figure 24, Figure 25, and Figure 26.

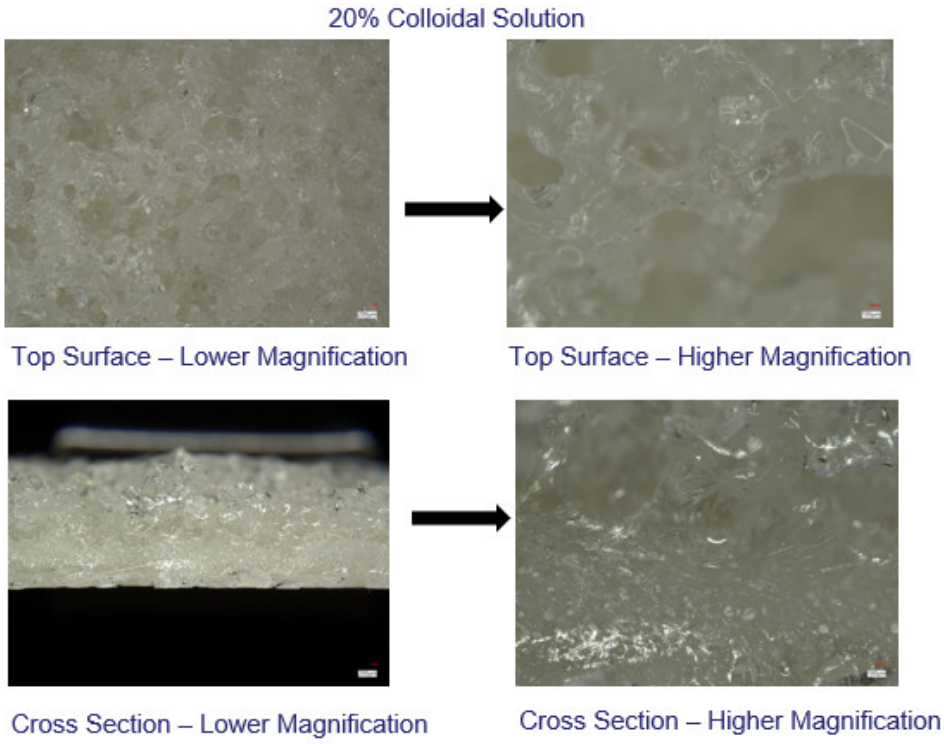

Figure 23. Formulation 2 with 20% colloidal solution

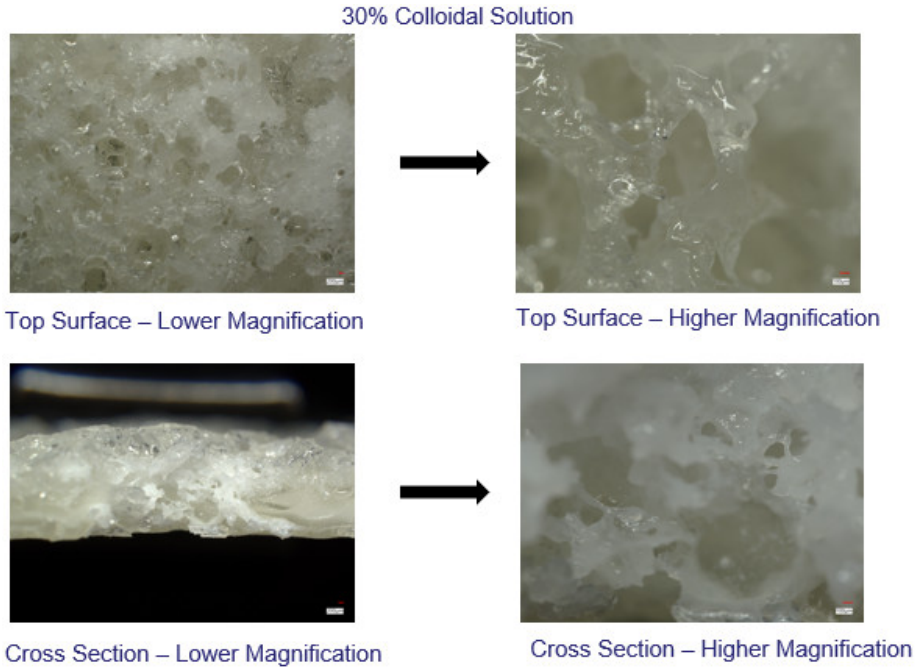

Figure 24. Formulation 2 with 30% colloidal solution

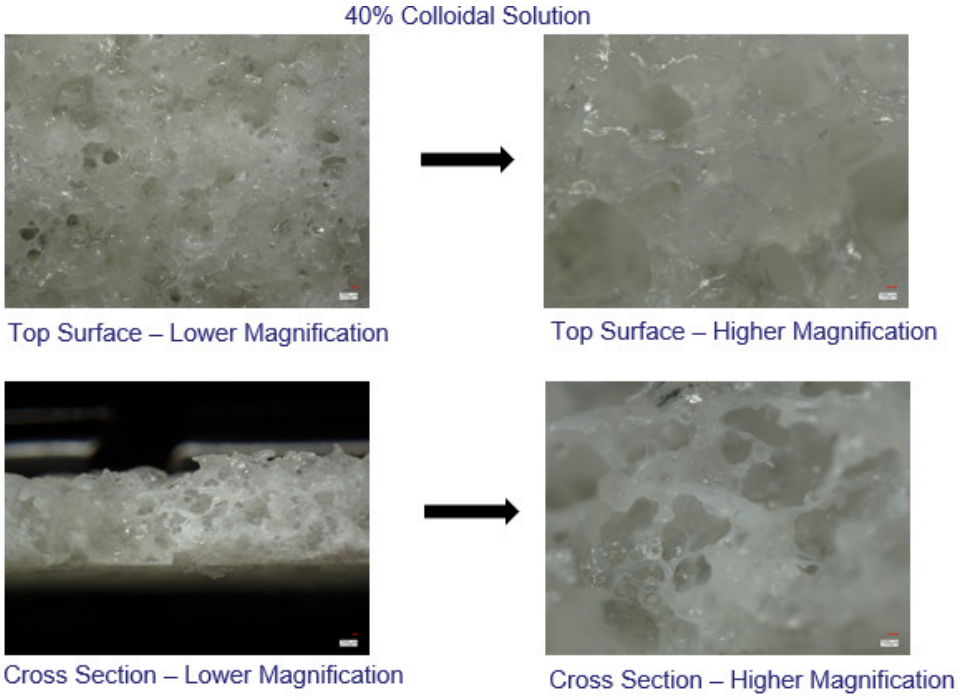

Figure 25. Formulation 2 with 40% colloidal solution

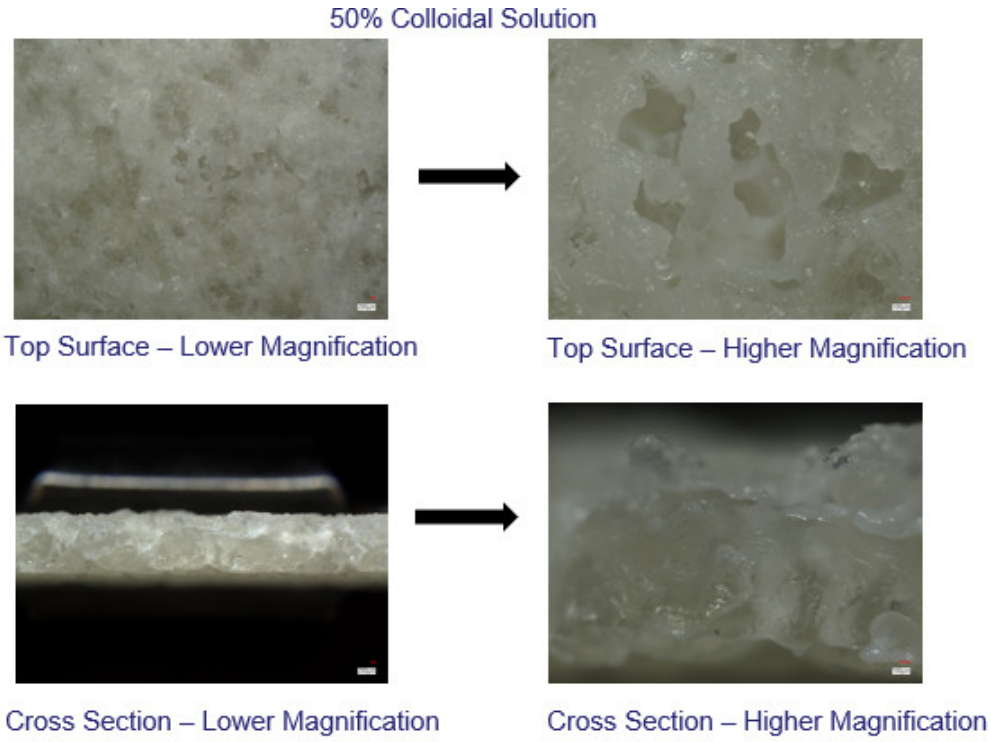

Figure 26. Formulation 2 with 50% colloidal solution

Each sample for 20-50% colloidal solution exhibits signs of open cell porous structures. The density and porosity of each sample are shown in
Table 4, where the density of INF-114 is 1.14 g/cc.

Table 4. Density and Porosity of INF open cell samples.

	Density (g/cc)	**Porosity (%)**
20% Colloidal Solution	0.705	38
30% Colloidal Solution	0.573	50
40% Colloidal Solution	0.510	55
50% Colloidal Solution	0.465	59

The porosities obtained for each sample show a higher percentage than the percentage of the internal phase used from the colloidal solution. This is consistent with all samples, which could be attributed to the nature of the open cell structures. Since these structures have interconnected pores, the process by which the open cell structure forms may introduce additional void space due to the geometry of the connections between pores. The stress-strain plot of these structures is shown in Figure 27.

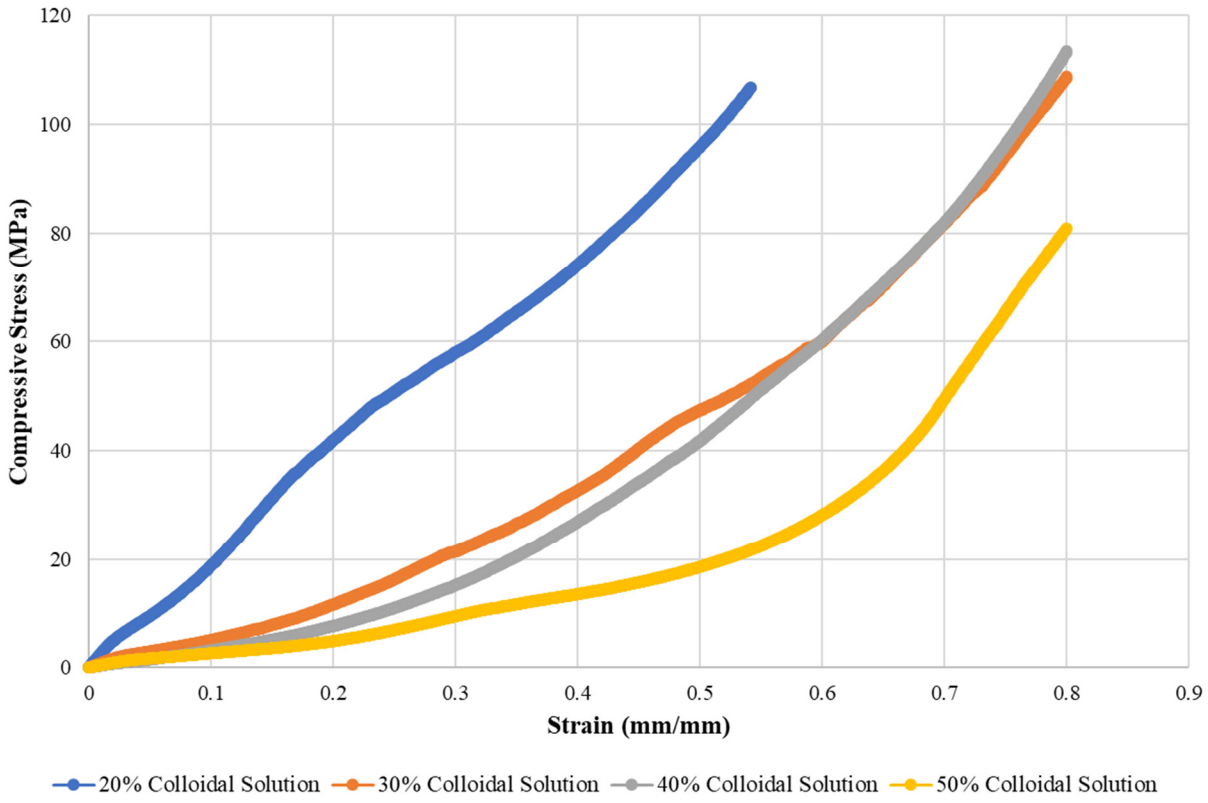

Figure 27. Stress-strain plot of open cell INF samples

The stress-strain plot shown in Figure 27 shows that the foams go straight to densification. This means that they are unable to bear loads and instead densify with increasing compressive stress. The modulus also decreases with increasing internal phase of the colloidal solution, as seen in Table 5.

Table 5. Modulus data for INF open cell samples

Sample	Modulus (GPa)
20% Colloidal Solution	0.2820
30% Colloidal Solution	0.0879
40% Colloidal Solution	0.0420
50% Colloidal Solution	0.0413

3.3.3.7 Closed Cell Foam Study

Closed cell foams were observed through the fabrication process involving EPON 815C and EPIKURE 3245 using Formulation 3. This formulation entails adding EPON 815C with EPIKURE 3245, mixing the solution, and then introducing and mixing the surfactant (Span® 20 or 80). TM-50 colloidal silica was added in the final step in either 1.5 g or 3 g amounts. The curing profile involved a temperature ramp to 80 °C that was held for 2 hours, then ramped to 100 °C and held for another 2 hours, and then ramped to 110 °C and held for 30 mins. These porous structures have pores that are encapsulated by their epoxy matrix, as shown in Figure 28 and Figure 29.

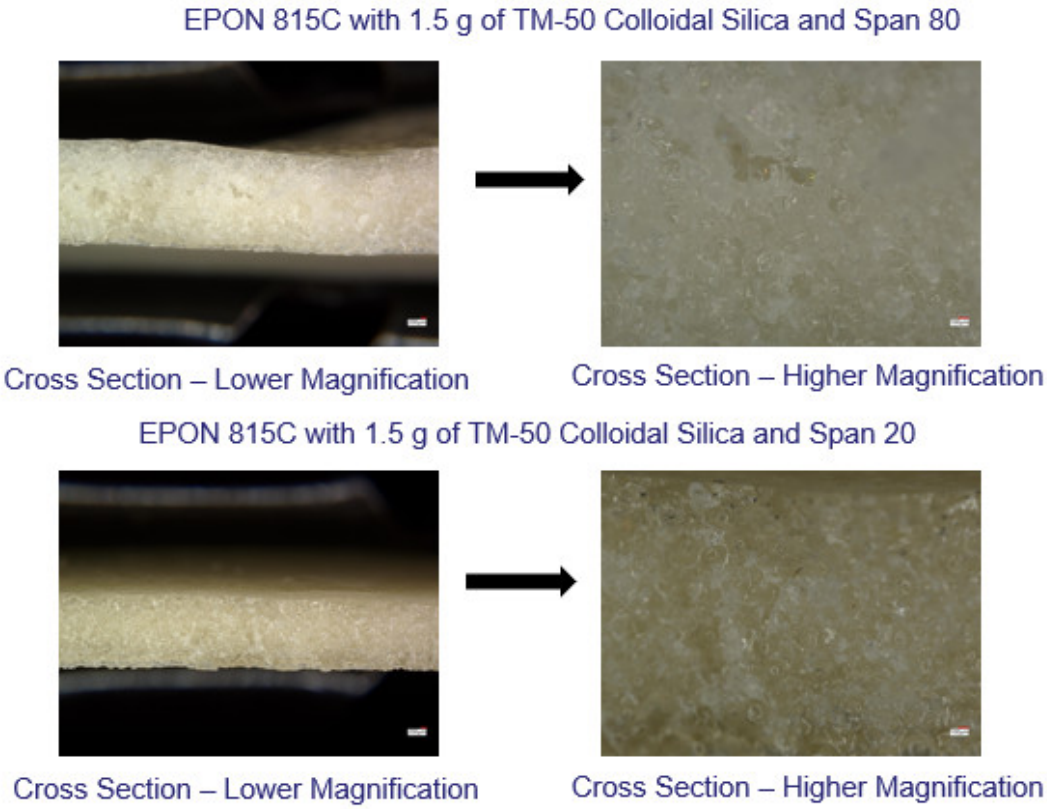

Figure 28. EPON 815C closed cell foam with 1.5 g of TM-50 colloidal silica

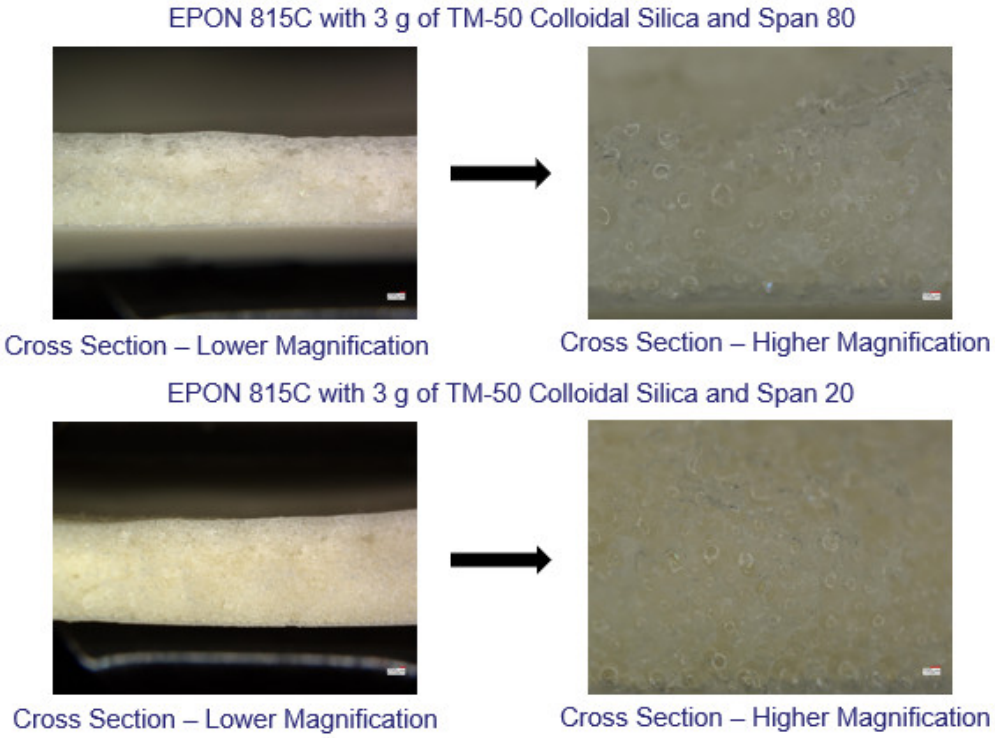

Figure 29. EPON 815C closed cell foam with 3 g of TM-50 colloidal silica

The density and porosity of each sample are shown in Table 6, where the density of EPON 815C is 1.13 g/cc.

Table 6. Density and porosity of EPON 815C closed cell structures.

EPON 815C with:	Density (g/cc)	Porosity (%)
1.5 g of TM-50 Colloidal Silica and a Span 80	1.012	10
1.5 g of TM-50 Colloidal Silica and Span 20	0.728	36
3 g of TM-50 Colloidal Silica and Span 80	0.435	62
3 g of TM-50 Colloidal Silica and Span 20	0.376	67

The porosity data shows a dramatic increase between using 1.5 g and 3 g of colloidal silica for the same amount of epoxy. The underlying mechanism behind this increase needs to be studied and verified, which if consistent, could provide interesting applications for tailoring highly porous foams with minimal water input as the internal phase. The stress-strain plots for these samples are shown in Figure 30.

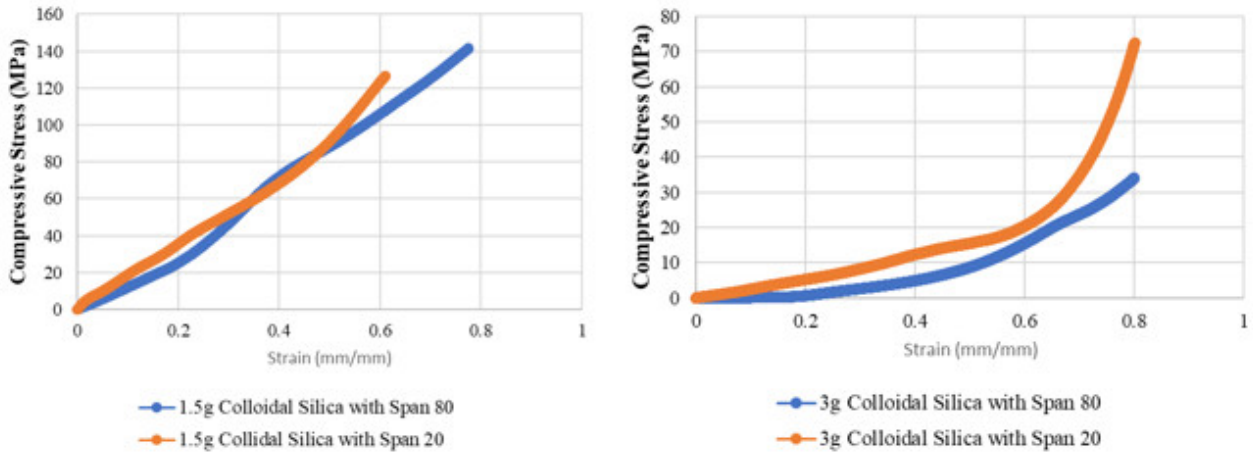

Figure 30. Stress-strain plot for EPON 815C closed cell samples

The closed cell samples, like their open cell counterparts also densify and are unable to hold loads. The modulus data is shown in Table 7.

Table 7. Modulus data for EPON 815C closed cell samples

	Modulus (GPa)	
The surfactant used in the sample	1.5g Colloidal Silica	3g Colloidal Silica
Span 80	0.137	0.000345
Span 20	0.319	0.028

This comprehensive research journey has yielded valuable insight into the synthesis, characterization, and optimization of porous epoxy materials through emulsion polymerization. It was found that the order in which Part B is added plays an important role in achieving successful emulsions. It was only after the mixing protocol was changed in adding Part B in the final step that led to meaningful open and closed cell porous structures. Additionally, using a low-viscous resin in INF-114 yielded open cell foams as opposed to EPON 815C, which yielded closed cell foams. Both sets of foams densify upon compression loading, with EPON 815C exhibiting crazing phenomenon post compression tests.

In conclusion, this research provides a comprehensive foundation for the design and fabrication of tailored porous epoxy materials. The insights gained from the study's multifaceted approach hold

substantial promise for applications spanning industries such as aerospace, automotive, and biomedical engineering. By bridging the gap between formulation, curing, and material analysis, this research facilitates the development of materials optimized for specific applications. The knowledge gleaned from this research serves as a cornerstone for future advancements in the realm of porous materials.

3.4 Accomplishments

A method to create porous epoxy polymers using an emulsion templating method was developed. Process and formulation variables, including water content, epoxy type, surfactant type, and mixing protocol, that can be used to tune pore size and morphology and mechanical properties, were investigated. This research provides a comprehensive foundation for the design and fabrication of tailored porous epoxy materials.

Previous work on using ABC as a porogen was expanded to other materials of interest, such as epoxies and polyurethanes. It was determined that epoxy foams contain pores the same size and shape of the ABC, but polyurethane foams act more like a blown foam with the pores being larger and more spherical than the ABC used as a pore former. Both behaviors could be of interest in different applications.

A method to make phenolic microballoons using a commercial off-the-shelf spray dyer was developed. Because the process temperatures were lower in the commercial spray dryer than in prior work, the formulation had to be tuned. Using an acid catalyst and a faster curing resin, KU was able to make phenolic microballoons at the lower temperature conditions. This method could potentially be adapted to make microspheres out of other materials of interest.

References

[1] Laura Cummings, *Next Generation Pore Formers PDRD* (Final Report). UNCLASSIFIED. FM&T: NSC-614-4854, June 2023.

APPENDIX A. GLOSSARY OF ACRONYMS/ABBREVIATIONS

The following table provides an alphabetical list of acronyms and abbreviations referenced in the report.

Acronym	Description
ABC	Ammonium Bicarbonate
ABCG	Ground Ammonium Bicarbonate
ABC45S	Ammonium Bicarbonate Sieved to 45 microns
AM	Additive Manufacturing
AVE	Advanced Video Extensometer
DI	Deionized
KCNSC	Kansas City National Security Campus
KU	University of Kansas
LANL	Los Alamos National Laboratory
LVDT	Linear Variable Differential Transformer
MPa	Megapascals
OU	University of Oklahoma
PDMS	Polydimethyl siloxane
PDRD	Plant Directed Research and Development
PU	Polyurethane
SEM	Scanning Electron Microscopy
UTS	Ultimate Tensile Strength

APPENDIX B. DISTRIBUTION

Internal

Recipient	Department	Email
Dakota Even	896	deven@kcnsc.doe.gov
David Rotert	894	drotert@kcnsc.doe.gov
Jamie Messman	863	jmessman@kcnsc.doe.gov
Jeff Jones	291	jjones10@kcnsc.doe.gov
Laura Cummings	896	lcummings2@kcnsc.doe.gov
Logan Wilkins	291	lwilkins@kcnsc.doe.gov
Maria LaGasse	896	mlagasse@kcnsc.doe.gov
Matt Selter	894	tselter@kcnsc.doe.gov
Records Management	011	recordcenter@kcnsc.doe.gov
Sabrina Torres	896	storres@kcnsc.doe.gov
Steven Patterson	897	spatterson@kcnsc.doe.gov
Taylor Schwahn	896	tschwahn@kcnsc.doe.gov

External

Recipient	Company	Email
Gary Gladysz	LANL	gladysz@lanl.gov
Rachel Collino	LANL	rcollino@lanl.gov

Kansas City National Security Campus
14520 Botts Road | Kansas City, MO 64147

KANSAS CITY NSC National Security Campus

The Department of Energy's Kansas City National Security Campus is managed and operated by Honeywell Federal Manufacturing & Technologies, LLC under contract number DE-NA0002839